Intraband and interband decomposition of high-order-harmonic spectra from bulk GaSe by an *ab-initio* simulation

Yasushi Shinohara[1], Keisuke Kaneshima[2], Kengo Takeuchi[2], Nobuhisa Ishii[2], Kotaro Imasaka[3], Tomohiro Kaji[3], Satoshi Ashihara[3], Jiro Itatani[2], and Kenichi L. Ishikawa[1]

[1]*School of Engineering, The University of Tokyo, 7-3-1 Hongo, Bunkyo-ku, Tokyo 113-8656, Japan,*
[2]*Institute for Solid Sate Physics, The University of Tokyo, 5-1-5 Kashiwanoha, Kashiwa, Chiba 277-8581, Japan,*
[3]*Institute of Industrial Science,, The University of Tokyo, 4-6-1 Komaba, Meguro-ku, Tokyo 153-8505, Japan*
shinohara@atto.t.u-tokyo.ac.jp

Abstract: We have developed an *ab-initio* simulation for high-order-harmonic generation from bulk GaSe. The simulation shows even-order harmonics are exclusively generated from the interband current while odd-order ones are dominated by intraband current below the band-gap.

OCIS codes: 190.7110 (Ultrafast nonlinear optics), 320.7130 (Ultrafast processes in condensed matter, including semiconductors).

1. Introduction

High-order harmonic generation (HHG) from bulk crystal has been intensively investigated by both experimental and theoretical approaches [1–3]. One of the most striking differences from gas-phase HHG is intraband contribution to HHG which is not described by the three-step picture. An analysis by separating intraband and interband contribution by theoretical simulation gives us a further insight to understand the funramental processes in solid HHG.

We have recently measured high-order harmonic (HH) spectra from bulk GaSe with resolving their polarization to the direction parallel or perpendicular to the linearly-polarized drive field. One of the most non-trivial results of this experiment is the presence of the third harmonic component in the direction perpendicular to the drive field, which is not explained by the third-order susceptibility. We perform an *ab-initio* simulation of solid HHG and compare the results to corresponding experiments. Furthermore, we elucidate the roles of two contributions, intraband current and interband polarization, to HH spectra by decomposing the induced current into these two sources.

2. Theoretical framework

We have developed an *ab-initio* theoretical framework based on time-propagation of a density matrix, $\hat{\rho}$,

$$\frac{\mathrm{d}}{\mathrm{d}t}\hat{\rho} = \frac{1}{i\hbar}\left[\hat{\rho}, \hat{h}(t)\right], \quad \hat{h}(t) = \hat{h}_0 + \frac{1}{m}\hat{\boldsymbol{p}}\cdot\boldsymbol{A} + \frac{1}{2m}\hat{\boldsymbol{A}}^2 + \hat{\Sigma} \tag{1}$$

where $\hat{h}_0$, $\boldsymbol{A}$, and $\hat{\Sigma}$ are a one-body field-free Hamiltonian, time-dependent vector potential, and a self-energy term respectively. This approach is the same as the semiconductor Bloch equation [4] with the independent particle approximation but in the velocity gauge rather than the length gauge. Each sampling point in the Brillouin zone is independently solved because of the velocity gauge. We solve the equation using the momentum matrix elements evaluated with orbitals derived from the self-consistent solution of the density-functional theory (DFT) with local-density approximation (DFT-LDA). We perform DFT-LDA calculation by using the elk code [5] with experimentally-determined lattice geometry of GaSe. The DFT-LDA band gap, 1.2 eV, is widened by an amount 0.8 eV to adjust it to the experimental value of 2.0 eV, by including a scissors operator as the self-energy term. This simulation requires dense Brillouin zone sampling to obtain converged results. We use $64 \times 64 \times 12$ grids for the sampling and 103 bands as the active space in the time-propagation.

We take real-time propagation of Eq. (1) under given A-field then obtain induced current density as $\boldsymbol{J}(t) = \mathrm{tr}\left(\hat{\rho}\hat{\boldsymbol{v}}\right)/V_{\mathrm{cell}}$, where $\hat{\boldsymbol{v}}$ is the velocity operator and V_{cell} is the cell volume. A HH spectra is obtained as a power spectrum

of the Fourier transform of the current times frequency square as $I_{\mathrm{HHG}}(\omega) = \omega^2 |J(\omega)|^2$. We evaluate the intraband current density as the diagonal contribution of the velocity operator in terms of instantaneous eigenfunction, indexed by α and β, of the time-dependent Hamiltonian,

$$\boldsymbol{J}_{\mathrm{intra}}(t) = \frac{1}{V_{\mathrm{cell}}} \sum_{\alpha \boldsymbol{k}} \langle \alpha \boldsymbol{k}(t) | \hat{\boldsymbol{v}} | \alpha \boldsymbol{k}(t) \rangle \rho^{\boldsymbol{k}}_{\alpha\alpha}(t), \quad \hat{h}(t) | \alpha \boldsymbol{k}(t) \rangle = e_{\alpha \boldsymbol{k}} | \alpha \boldsymbol{k}(t) \rangle, \quad \rho^{\boldsymbol{k}}_{\alpha\beta} = \langle \alpha \boldsymbol{k}(t) | \hat{\rho} | \beta \boldsymbol{k}(t) \rangle . \tag{2}$$

The interband current density is obtained as a residual from total one, $\boldsymbol{J}_{\mathrm{inter}} = \boldsymbol{J} - \boldsymbol{J}_{\mathrm{intra}}$. HH spectrum from each contributions is obtained by the same manner as for $I_{\mathrm{HHG}}(\omega)$.

3. Results and discussion

In the experiment, the basal plane of GaSe is exposed to linearly polarized mid-infrared (MIR) pulses (5 μm, 200 fs, 10.0 MV/cm in the crystal), namely the drive field vectors always on the basal plane. The polarization components of HH spectra are selected by a wire-grid polarizer. Angular dependence with respect to the crystal axis is measured by rotating the sample around z-axis in steps of 5°. We define the rotation angle ϕ as in Fig. 1(a). In the simulation, a similar drive field is chosen at 4.96 μm, 10.0MV/cm, with a duration of 160 fs. Polarization of HH spectrum is calculated and the direction of the drive electric field is changed in steps of 5° as well.

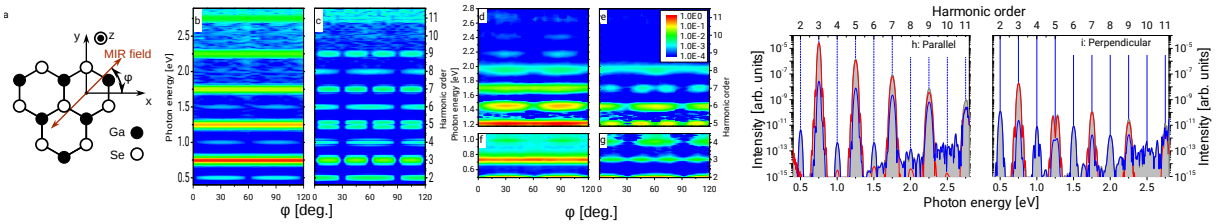

Fig. 1. (a) Top view of the GaSe crystal and the definition of the orientation angle, ϕ, with respect to the MIR field direction. The parallel (b) and perpendicular (c) polarization components of the HH as a function of the rotation angle for the simulation. The parallel (d,f) and perpendicular (e,g) polarization components for the experiment. (h) HH spectrum of the parallel components (shaded area) at $\phi = 15°$ and its decomposition into the intraband current (red curve) and the interband current (blue curve). (i) The same plot as (h) for the perpendicular components.

Fig. 1.b-c and Fig. 1.d-g shows the comparison of angle-dependent HH spectrum. The perpendicular components for odd-order harmonics, in both the experimenta and simulation, show 30-degree periodicity, which is inconsistent with the third-order nonlinear susceptibility. This non-trivial observation is understood as the fifth-order nonlinear process to produce third harmonics as $3\omega = 4\omega - \omega$ by our simulations and tensor analysis.

Decomposition of HH spectrum into intraband and interband contributions is shown in Fig. 1.h-i. In both components, the odd harmonics are predominantly produced by the interband current. At higher orders, especially above the band gap, the contribution of the interband polarization catches up with that of the intraband current. On the other hand, the interband polarization exclusively contributes to all even harmonics. This result reflects the fact that the band dispersion has always inversion symmetry to suppress the generation of even-order harmonics by intraband current, while the interband polarization can contain both even and odd-order harmonic components.

References

1. S. Ghimire, et al., "Observation of high-order harmonic generation in a bulk crystal," Nat. Phys. **7**, 138 (2011).
2. F. Langer, et al., "Symmetry-controlled temporal structure of high-harmonic carrier fields from a bluk crystal," Nat. Photon. **11**, 227 (2017).
3. T. Ikemachi, et al., "Trajectory analysis of high-order-harmonic generation from periodic crystals," Phys. Rev. A **95**, 043416 (2017).
4. M. Lindberg and S. Koch, "Effective Bloch equation for semiconductors," Phys. Rev. B **38**, 2242 (1988).
5. http://elk.sourceforge.net/.